

# Mechanical means for temperature compensation of planar diffractive optical interconnects: feasibility study

Yehoshua Socol

College of Judea and Samaria  
Department of Electrical and Electronics Engineering  
Ariel, Israel  
E-mail: socol@yosh.ac.il

**Abstract.** Planar diffractive optical interconnects have many advantages, however, their inherent chromaticity leads to temperature instability due to the wavelength shift of laser diodes' radiation. This shift can be compensated if the optical interconnect is bended in an appropriate direction with curvature proportional to the relative wavelength shift. The bending can be performed by attaching an additional plate to the element with a different thermal expansion coefficient. Theoretical analysis and ray tracing are reported.

© 2006 Society of Photo-Optical Instrumentation Engineers.  
[DOI: 10.1117/1.2189869]

Subject terms: interconnects; thermal effects; optical communications.

Paper 050575LR received Jul. 13, 2005; revised manuscript received Jan. 27, 2006; accepted for publication Feb. 6, 2006; published online Apr. 3, 2006.

In the semiconductor industry, there is a continually aggravating problem of increasing communication volume. Optical interconnection technology is seen as a prime option for solving this problem.<sup>1,2</sup> In planar optical interconnects (POI) light is injected (by an in-coupling optical element) into a transparent slab (light guide) at a total internal reflection angle ( $\psi$  in Fig. 1) and propagates along it until it meets an out-coupling optical element and goes to the detector. Diffractive lenses as coupling optical elements have many advantages<sup>3-5</sup> and have been suggested also in the context of quasi-optics<sup>6</sup> for rapidly expanding terahertz technology.<sup>7</sup> However, their intrinsic dependence of optical properties on the wavelength—chromaticity—poses difficult problems.<sup>8</sup> Chromaticity leads also to temperature instability. Namely, the wavelength of semiconductor lasers is temperature-dependent. Temperature change causes wavelength shift, therefore the laser beam as deflected by the diffractive in-coupling optical element deviates from its desired path and can miss the out-coupling element. For example, for a typical 850-nm vertical-cavity surface-emitting lasers (VCSEL) source the wavelength shift is  $d\lambda/dT=0.06$  nm/K,<sup>9</sup> i.e., relative wavelength shift is  $(1/\lambda)(d\lambda/dT) \sim 7 \times 10^{-5}$  K<sup>-1</sup>. If POI was assembled at 20°C, the working temperature is 140°C (*Max3905* from Dallas Semiconductors, e.g.), and the POI length is 10 cm, the resulting beam deviation is about 1.7 mm (see below the calculation). This temperature instability is specific for diffractive POI since other thermal effects are much less:

e.g., for fused silica the explicit refraction index temperature dependence is  $-3 \times 10^{-6}$  K<sup>-1</sup>.<sup>10</sup> The implicit temperature dependence (due to the refraction index wavelength dependence  $dn/d\lambda$  and the laser wavelength shift  $d\lambda/dT$ ) is even smaller:  $dn/d\lambda=4 \times 10^{-5}$  nm<sup>-1</sup>,<sup>10</sup> leading to  $dn/dT=(dn/d\lambda)(d\lambda/dT)=2.4 \times 10^{-7}$  K<sup>-1</sup>.

We propose to fix this problem by bending POI in accordance to the temperature change. We suppose that POI and the laser have the same temperature since they are close to each other. A simple bending scheme is absolutely passive and implies attaching to POI a second plate, having different thermal expansion coefficient (in mass production, the attachment may be done by lamination technology<sup>11</sup>). The curvature of this bending is proportional to the temperature change (as long as the thermal expansion can be considered as linear with temperature). As long as the laser wavelength shift can be also considered proportional to the temperature change, the bending curvature is proportional to the wavelength shift. Thus, with appropriate proportionality between the bending curvature and the wavelength shift, the bending will cause the diffracted beam to propagate along nearly the same path for different wavelength.

Let us consider the problem quantitatively. At some reference temperature  $t_0$ , POI is strictly planar and the incident angle of the incoming beam is zero (Fig. 1). Let the propagation angle (within POI) be  $\psi$  (see Fig. 1). When temperature changes ( $t$ ), POI bends symmetrically in respect to perpendicular plane situated just in the middle between the input and output diffractive elements (Fig. 2). The incident angle  $\alpha$  becomes nonzero since the laser beam direction does not change in the lab frame. However, the bending curvature can be tuned in such a way that the propagation angle  $\psi$  retains its original value (locally in the incidence/refraction point) due to the incident angle change. We show now how this tuning is achieved.

First, we derive the beam displacement as function of wavelength  $\lambda$  shift. For the reference radiation wave vector  $k_0=2\pi/\lambda_0$ , incident angle  $\alpha_0=0$ , grating vector  $K=2\pi/\Lambda$  ( $\Lambda$  is grating period), propagation angle  $\psi$ , and propagation vector  $\vec{r}$  we have<sup>12</sup>

$$r_x = K, \quad \sin \psi = r_x/nk_0 = K/nk_0 = \lambda_0/n\Lambda \quad (1)$$

[see Fig. 3(a)]. For another wavelength (wave vector  $k$ ), the propagation angle  $\psi'$  is different [Fig. 3(b)]. We define relative beam displacement as  $\Delta l/l = (\tan \psi' - \tan \psi)/\tan(\psi)$ , since in one "period" (bounce-back) the

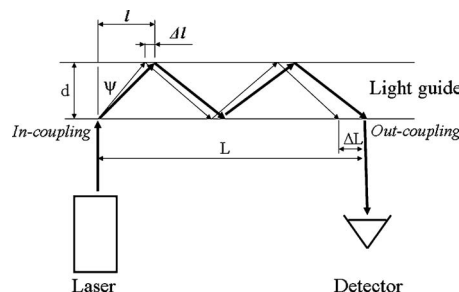


**Fig. 1** Planar optical interconnect layout. Initial (thick line) and displaced due to the laser-wavelength-shift (thin line) beams are shown.

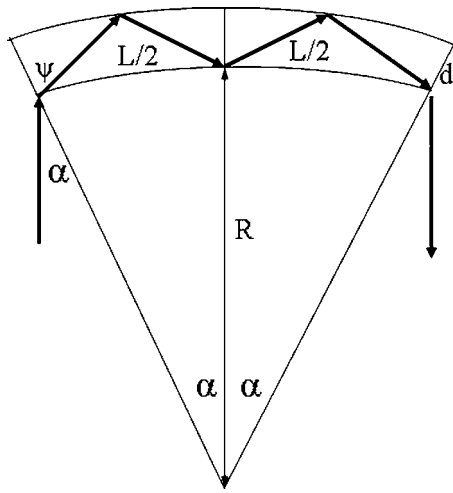


**Fig. 2** Layout of a bended POI:  $\alpha$  is the incidence angle of the laser beam,  $\psi$  is its propagation angle,  $t$  is the POI thickness, and  $R$  is the POI bending radius. The shown bending direction corresponds to  $\lambda < \lambda_0$ , i.e., a shift toward shorter wavelength (i.e., lower temperatures).

beam covers longitudinal distance  $l = 2d \tan \psi$  (Fig. 1), where  $d$  is the light guide thickness. We suppose that the relative displacement is rather small and consider equal numbers of “periods.” To calculate this relative displacement, we define the wavelength relative change as

$$\delta = (k - k_0)/k_0 \approx (\lambda_0 - \lambda)/\lambda_0, \quad (2)$$

where  $\delta$  is defined as positive for shorter wavelengths (longer wave vectors) in respect to the basic one at reference temperature  $t_0$ . Calculation of relative beam displacement in the first order in respect to  $\delta$  yields:  $d(\tan \psi)/d\lambda = [d(\tan \psi)/d(\sin \psi)][d(\sin \psi)/d\lambda]$ . As for the second term, we have from Eq. (1)  $d(\sin \psi)/d\lambda = 1/n\Lambda$ , and for the first one  $d(\tan \psi)/d(\sin \psi) = d(\tan \psi)/d\psi : d(\sin \psi)/d\psi$ , yielding finally

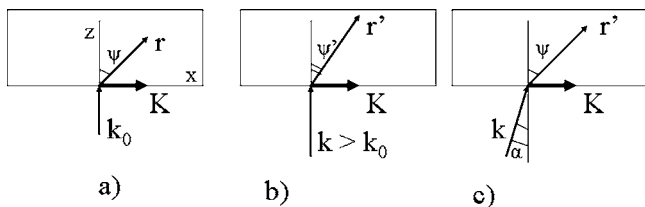


**Fig. 3** Beam deviation as a result of wavelength shift and its correction. The laser beam with wave vector  $k_0$  enters the interconnection plate along the  $z$ -axis (the incidence angle  $\alpha = 0$ ) at reference temperature  $t_0$ ;  $k_0$ ,  $k$ , and  $r$ ,  $r'$  are the incident and refracted wave vector lengths at reference temperature  $t_0$  and at different temperature  $t$  correspondingly, and  $K$  is the grating vector of the diffractive optical element. (a) Reference temperature  $t_0$ ; the propagation angle is  $\psi$ ; (b) temperature changes to  $t$ , incident wave vector is longer  $k = k_0(1 + \delta)$ , propagation angle is  $\psi' < \psi$ ; (c) temperature  $t$ , after bending: the incidence angle is  $\alpha$ ; due to the incident beam tilt, the propagation angle is again  $\psi$ .

$$\frac{\Delta l}{l} \approx \frac{\Delta \lambda}{\lambda \cos^2 \psi}. \quad (3)$$

Since usually  $\psi \sim \pi/4$ ,  $\Delta l/l \sim 2\delta$ . For example, taking the relative wavelength shift  $(1/\lambda)(d\lambda/dT) \sim 7 \cdot 10^{-5} \text{ K}^{-1}$  (for 850-nm VCSEL, as mentioned above) and temperature shift  $120^\circ\text{C}$ , we get  $\Delta l/l \sim 0.017$ , i.e., for  $L = 100 \text{ mm}$ ,  $\Delta L = L \cdot \Delta l/l = 1.7 \text{ mm}$ .

In order to correct this deviation we want to get the same propagation angle  $\psi$  at a different temperature  $t$ . To achieve this we must take nonzero incident angle  $\alpha$  [Fig. 3(c)]. Therefore  $r'_x = K + k \sin \alpha$  and  $\sin \psi = r'_x/nk$ . We obtain

$$\frac{K}{nk_0} = \frac{K + k \sin \alpha}{nk}. \quad (4)$$

Substituting Eq. (1) into this equation and making use of  $\delta$  defined in Eq. (2) yields

$$\sin \alpha = (\delta/(1 + \delta))n \sin \psi. \quad (5)$$

For bending curvature radius  $R$  and the interconnect length  $L$  (distance between input and output) we obviously have (Fig. 2)  $\alpha = L/2R$ . Now we have

$$\epsilon = 2d\alpha/L, \quad (6)$$

where  $\alpha$  is given by Eq. (5),  $\epsilon$  is defined as  $\epsilon = d/R$ , and  $d$  is the POI thickness. Positive values of dimensionless curvature  $\epsilon$  and radius  $R$  correspond to curvature center from the laser/detector side (see Fig. 2).

Let us calculate now the change of the beam trajectory in the curved element is respect to the original planar. Consider one beam reflection. In Fig. 4,  $\angle EAO = \pi - \psi$ . In the triangle  $\Delta EAO$ ,  $\angle AEO = \pi - (\pi - \psi) - \beta = \psi - \beta$  (it should be noted here that the second incidence angle  $\angle AEO$  is smaller than  $\psi$  and can be below the total internal reflection threshold). In  $\Delta EBA$ ,  $\tan(\psi - \beta) = AB/EB$ . Considering circumference with origin  $O$  we get  $EB = EC + CB = d + R(1 - \cos \beta)$  and  $AB = R \sin \beta$ . We have therefore

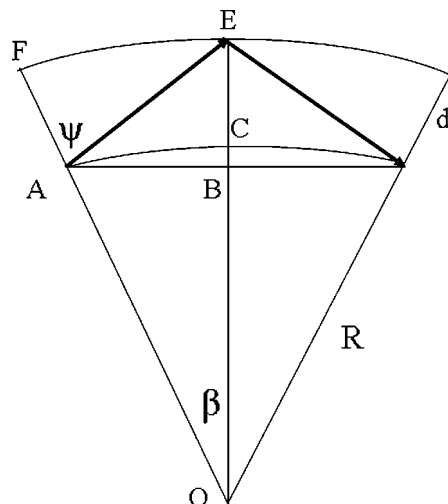


**Fig. 4** Light propagation in bended POI—1 “period” (bounce-back). Notation for derivation of Eqs. (7) and (8).

$$d + R(1 - \cos \beta) = R \sin \beta \cdot \cot(\psi - \beta) \quad (7)$$

and finally

$$\epsilon + 1 - \cos \beta = \sin \beta \cot(\psi - \beta). \quad (8)$$

We solve this equation by iterations, supposing that for small  $\epsilon$ ,  $\beta$  will be also small. Expanding Eq. (8) in respect to  $\beta$  and keeping the leading term only, we have

$$\beta_1 = \epsilon \tan \psi. \quad (9)$$

Within this approximation, the distance between input and output of 1 bounce-back is  $2R\beta_1 = 2R(d/R)\tan \psi = 2d \tan \psi$ , exactly as in the planar case (Fig. 1). Though the actual beam deviation in space is nonzero due to the bending, it is of second order in respect to  $\delta$ . However, actually there is linear with  $\delta$  deviation. In order to estimate it, we make the second iteration. Substituting  $\beta = \beta_1 + \beta_2$  and keeping the leading order of  $\beta_2$  yields

$$\beta_2 = -\frac{3 + \cos 2\psi}{2 \sin 2\psi} \beta_1^2. \quad (10)$$

As mentioned above, the unperturbed input-output distance is  $l = 2d \tan \psi = 2R\beta_1$ , and after wavelength shift and correction bending this distance is  $2R(\beta_1 + \beta_2)$ . So the first order approximation to the relative beam displacement is

$$\frac{\Delta l}{l} = \frac{\beta_2}{\beta_1} = -\epsilon \frac{3 + \cos 2\psi}{2 \sin 2\psi} \tan \psi. \quad (11)$$

Thus  $\Delta l/l \sim \epsilon \sim \delta \cdot d/L$  [Eqs. (5) and (6)].

Without bending, as mentioned before [Eq. (3)], the relative beam displacement is  $\Delta l/l \sim 2\delta$ . Therefore the wavelength-shift-caused beam deviation is reduced by factor of  $\sim d/L$ , i.e., usually above one order of magnitude. Figure 5 presents ray tracing results of the beam deviation as function of wavelength change—with and without compensation by means of POI bending. Exact ray tracing [numerical solution of Eq. (8)] results are indistinguishable from the approximation [Eq. (11)].

The proposed scheme works only when the source and the detector are situated from one side of POI, but this seems to be the common case. One can realize this scheme for rectangular or circular arrays of sources/detectors. In the latter case, each pair source-detector should be situated diametrically and the bending curvature center should be at the line normal to the array circle and crossing its center. Linear behavior of curvature in respect to temperature should take place also in this case.

Finally, speaking about diffractive optical elements for VCSEL, it should be mentioned that there is an unavoidable spread of nominal VCSEL wavelengths (at a given temperature) from one laser array (chip) to another of usually up to around 10 nm or more. The problem of this “bias” may be solved at the assembling stage by off-axis adjusting of the laser array, as in Fig. 3(c). The off-axis

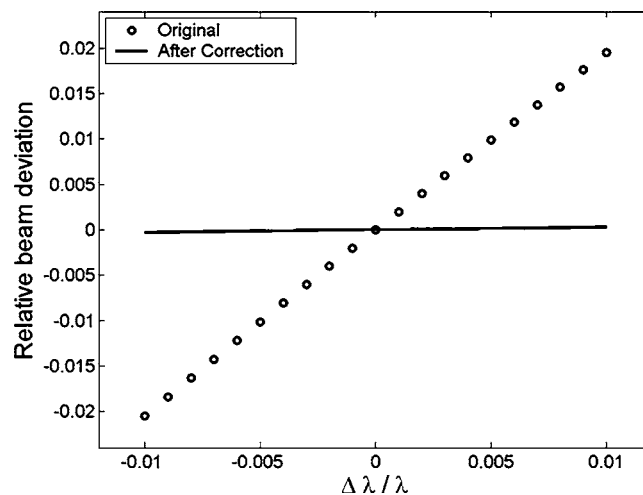


**Fig. 5** Ray tracing results for strictly planar [initial, Eq. (3)] and bended (after correction) planar optical interconnect. The bending radius fits the wavelength change. The results “after correction” obtained by exact solving of Eq. (8) and by the approximate formula in Eq. (11) are indistinguishable within the given scale. The parameters are:  $\psi = 45^\circ$ ,  $t = 0.1$  mm,  $L = 10$  mm.

angle  $\alpha$  is given by Eq. (5); its magnitude is about  $\alpha \sim \Delta \lambda / \lambda \sim 0.01$ . As far as  $\alpha \ll 1$ , the effects are linear and this adjusting should not affect the above results regarding the temperature compensation.

We are grateful to the anonymous referee, who made many valuable comments, leading to considerable improvement of this letter.

## References

1. M. Gruber, “Multichip module with planar-integrated free-space optical vector-matrix-type interconnects,” *Appl. Opt.* **43**(2), 463–470 (2004).
2. K. Banerjee, S. J. Souri, P. Kapur, and K. C. Saraswat, “3-D ICs: A novel chip design for improving deep-submicrometer interconnect performance and systems-on-chip integration,” *Proc. IEEE* **89**(5), 602–633 (2001).
3. Y. Amitai and J. W. Goodman, “Design of substrate-mode holographic interconnects with different recording and readout wavelengths,” *Appl. Opt.* **30**(17), 2376–2381 (1991).
4. J. Jahns and B. Acklin, “Integrated planar optical imaging-system with high interconnection density,” *Opt. Lett.* **18**(19), 1594–1598 (1993).
5. E. Socol, Y. Amitai, and A. A. Friesem, “Design of planar optical interconnects,” *Proc. SPIE* **2426**, 433–443 (1995).
6. J. M. Dai, S. Coleman, and D. Grischkowsky, “Planar THz quasi-optics,” *Appl. Phys. Lett.* **85**(6), 884–886 (2004).
7. J. Shan and T. F. Heinz, “Terahertz radiation from semiconductors,” *Top. Appl. Phys.* **92**, 1–56 (2004).
8. G. Minguez-Vega, M. Gruber, J. Jahns, and J. Lancis, “Achromatic optical Fourier transformer with planar-integrated free-space optics,” *Appl. Opt.* **44**(2), 229–235 (2005).
9. Z. Toffano, M. Pez, P. Desgreys, et al., “Multilevel behavioral simulation of VCSEL-based optoelectronic modules,” *IEEE J. Sel. Top. Quantum Electron.* **9**(3), 949–960 (2003).
10. N. Koshkin and M. Shirkevich, *Handbook of Elementary Physics*, Table 113, Mir Publishers, Moscow (1968).
11. S. Kalpakjian and S. R. Schmid, *Manufacturing Processes for Engineering Materials*, Prentice Hall, Englewood Cliffs, NJ (2002).
12. J. W. Goodman, *Introduction to Fourier Optics*, Roberts and Co. Publishers (2004).